INSTITUTE OF PHYSICS PUBLISHING PLASMA SOURCES SCIENCE AND TECHNOLOGY

Plasma Sources Sci. Technol. **10** (2001) 17–23 www.iop.org/Journals/ps PII: S0963-0252(01)17436-0

Time dependence of rotational state populations of excited hydrogen molecules in an RF excited plasma reactor

T Gans, V Schulz-von der Gathen and H F Döbele

Institut für Laser- und Plasmaphysik, Universität GH Essen, 45117 Essen, Germany

Received 17 July 2000, in final form 19 September 2000

Abstract

We report on time-dependent population distributions of excited rotational states of hydrogen in a capacitively coupled RF discharge. The common model to obtain the gas temperature from the rotational distribution is not applicable at all times during the discharge cycle due to the time dependence of the EEDF. The apparent temperature within a cycle assumes values between 350 K and 450 K for the discharge parameters of this experiment. We discuss the optimum time window within the discharge cycle that yields the best approximation to the actual temperature. Erroneous results can be obtained, in principle, with time-integrated measurements; we find, however, that in the present case the systematic error amounts to only approximately 20 K. This is due to the fact that the dominant contribution to the average intensity arises during that time window for which the assumptions underlying the analysis are best fulfilled. A similar analysis can be performed for N_2^+ rotational bands with a small amount of nitrogen added to the discharge gas. These populations do not exhibit the time variations found in the case of H_2.

1. Introduction

Capacitively and inductively coupled RF discharges bear considerable application potential. They are frequently applied in surface modification (cleaning, conditioning), the generation of microstructures (etching) and in layer deposition [1]. Emission spectroscopic methods are ideally suited to the control of these processes since the experimental requirements are comparatively modest. Important plasma parameters can be obtained, in principle, from emission spectroscopy (e.g. particle densities [2], particle temperatures [3] and electron energy distributions [4], etc). The reliable determination and control of the gas temperature is of particular importance, since this quantity plays a key role for many technically relevant plasma processes. The basic problem of emission spectroscopy of low-temperature non-equilibrium plasmas consists in extracting the required information with models based on atomic and molecular data.

In capacitively coupled RF discharges the densities of energetic electrons exhibit time dependences [5, 6]. This is clearly seen in time-resolved emission measurements, see figure 4(a) below, since the emission is mainly due to excitation by 'hot' electrons [7, 8]. The models used to infer plasma parameters from emission spectroscopy refer to the populations of levels from which optical emission is observed. If, therefore, the basic assumptions of these models describing the population and depopulation are not fulfilled throughout the full discharge cycle, it is possible that time-integrated measurements lead to erroneous results in these cases. It is, therefore, necessary to gain insight into the time dependence of the population dynamics which necessitates emission measurements with time resolution.

Time-resolved emission measurements on a time scale shorter than 10 ns (as required for the generally applied excitation frequency of 13.56 MHz) are not trivial at the comparatively low light levels. Conventional CCD cameras allow time-resolved measurements only with very intense emission lines, since the duration of the measurement would be otherwise too long for a stable plasma operation without long-term drifts. We now have the possibility, with the aid of a novel intensified CCD camera (LaVision Picostar HR), to shorten the time of observation by three orders of magnitude so that less intense emission lines can also be monitored with time resolution.

The Fulcher bands of H_2 are often availed to determine the gas temperature in hydrogen discharges. The corresponding spectral lines are located in a convenient spectral range (around 600 nm) and are relatively intense. The model which is applied

to infer the gas temperature will be explained below. The gas temperature is not expected to exhibit time dependences on a time scale of the RF period ($\tau_{RF} = 74$ ns) so that this quantity is well suited as a test for the time dependence of the basic model assumptions.

2. Experiment

The measurements are performed with a capacitively coupled RF discharge (CCRF discharge) similar to the 'GEC reference cell' [9]. The cooled parallel stainless-steel electrodes of diameter 100 mm are 25 mm apart. The plasma is generated with an RF power supply (Kenwood TS 140S) and a matching unit (ENI MW-10 D) at a frequency of 13.56 MHz in an asymmetric configuration with one electrode grounded. The power can be varied between 10 W and 100 W. The total gas pressure is determined with a capacitive gauge (Edwards Barocel 600) and is in the range between 10 Pa and 150 Pa. The basic gas flow (50 sccm) consisting of 99% H_2 with 1% argon is supplied by a mass flow controller (MFC). An admixture of N_2 is used in some experiments to allow, in parallel, the investigation of time dependences of excited N_2^+ rotational levels, which are also frequently applied to obtain information on the gas temperature [10, 11].

Knowledge of the intensity ratios within one rotational band is necessary to infer the rotational temperatures. It is advantageous to measure the intensities of the rotational lines simultaneously in order to avoid the influence of temporal drifts of the plasma or the experimental conditions. Diode line arrays or CCD cameras are therefore better suited as detectors than photomultipliers. CCD cameras have the additional advantage over diode arrays that the second dimension can provide, at the same time, axial spatial resolution. Gateable cameras allow time-resolved measurements by locking the gate to a fixed phase position within the exciting RF cycle. The intensities integrated over the gate time of 6 ns, for example, can be integrated over many RF cycles for this fixed phase setting. A variable delay between the fixed phase and the gate allows one to cover the complete RF cycle. The maximum repetition rate for consecutive gates is limited with conventional cameras to 10 kHz so that only every thousandth cycle can be utilized for the measurement. Therefore, in the case of weak lines, the durations of measurements have to be so long that stable experimental conditions are no longer warranted. A simple estimate for our experimental conditions can illustrate the situation. In order to record, with our equipment (that includes a 2m-spectrograph), the H_α emission from the discharge without time resolution an exposure time of about 100 ms is necessary. In order to perform a time-resolved measurement with the rotational lines that are weaker by approximately a factor of 200 ($v = 2$; $N = 4, 5$) with 12 time windows, 6 ns each, with a repetition rate of 10 kHz, the pertinent exposure would reach 1.5 months.

With the new camera (LaVision PicoStar HR) the repetition rate can be as high as 13.56 MHz so that each individual RF cycle can be utilized. The duration of the measurement is thus reduced by three orders of magnitude to about 1 h. This allows, for the first time, time-resolved measurements of the kind described, because over this time stable experimental conditions can be expected.

The light from the discharge is imaged with a combination of mirrors and lenses onto the entrance slit of a 2m-spectrograph (Jenoptik PGS 2, inverse dispersion 0.34 nm mm^{-1} with a 1302 grooves mm^{-1} grating). The CCD camera mentioned is mounted in its focal plane. On the active image array (13.2 mm × 8.8 mm; 576 × 384 pixel) about 4.5 nm of the emission spectrum can be recorded so that the first five lines of the hydrogen rotational band mentioned can be monitored in parallel. Figure 1 shows the schematic diagram of the experimental set-up.

3. Determination of the gas temperature

The model for the determination of the gas temperature is described in detail in [3]. The spontaneous emission intensity of a rovibronic transition ($n', v', N' \rightarrow n'', v'', N''$) is proportional, in the optically-thin case, to the product of the population density of the upper state $N_{n'v'N'}$ and the transition probability $A^{n'v'N'}_{n''v''N''}$:

$$I^{n'v'N'}_{n''v''N''} \propto N_{n'v'N'} A^{n'v'N'}_{n''v''N''}$$

where n describes an electronic state, v a vibronic state and N a rotational state. If the population of the upper state can be described by a Boltzmann distribution, $T_{rot}(n', v')$ governs the distribution in the following manner:

$$N_{n'v'N'} = c_{n'v'} g_{a,s} (2N' + 1) \exp\left(-\frac{E_{n'v'N'}}{kT_{rot}(n', v')}\right).$$

Here, $c_{n'v'}$ is a normalizing constant, $g_{a,s}$ is the degeneracy caused by the nuclear spin, $E_{n'v'N'}$ is the energy of the rovibronic level and k is the Boltzmann constant.

The rotational temperature can only be identified with the gas temperature, T_g, if the relaxation time for rotation in the excited state is much smaller than its radiation lifetime and the characteristic times of all other relaxation processes can lead to a redistribution. This is only warranted in the case of low-temperature non-equilibrium plasmas for small rotational quantum numbers of long-lived metastable states or of the ground state of molecules [12]. It is nevertheless possible, under certain conditions, to formulate, with the aid of a kinetic model for the population and the depopulation of excited levels, a relation between the rotational and the gas temperature. These conditions are as follows.

(1) The population distribution in the ground state $1s\,^1\Sigma_g^+$ obeys a Boltzmann distribution whereby the rotational temperature equals the gas temperature [13].
(2) The excited states are populated only via electron collisions from the ground state.
(3) The rate coefficients can be used in the adiabatic approximation. This is fulfilled for the Q-branches of the Fulcher-α system ($3p\,^3\Pi_u^- \rightarrow 2s\,^3\Sigma_g^+$) [3].
(4) The excitation without change of the rotational quantum number ($\Delta N = 0$) dominates, so that excitations with $\Delta N = \pm 2, \pm 4$, etc are negligible. This means that the rate coefficients are independent of the rotational quantum number [14].
(5) The effective lifetime of the excited state is independent of the rotational quantum number and is much shorter than the relaxation time of the rotational levels.

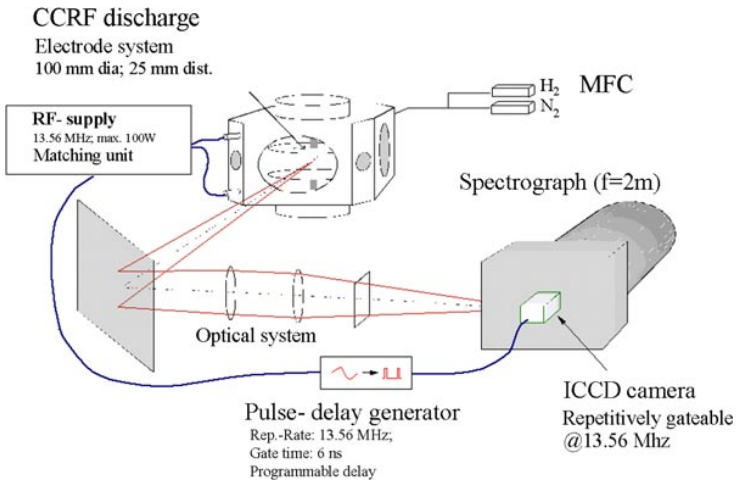

Figure 1. Experimental set-up of the discharge chamber and the electronic and optical systems for emission spectroscopy.

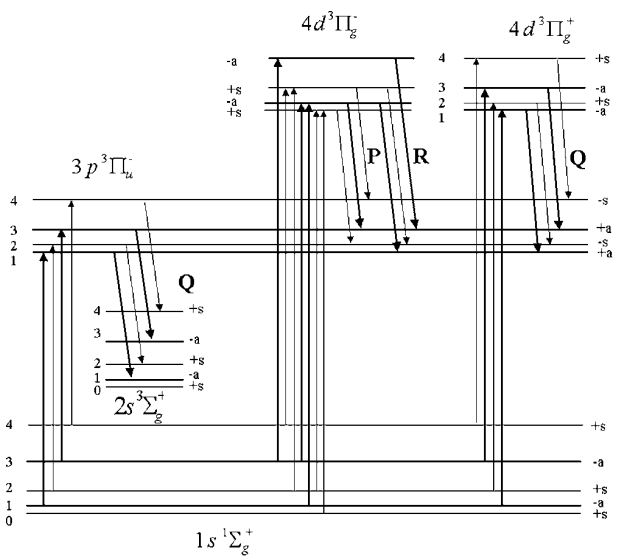

Figure 2. Term diagram illustrating the population mechanisms discussed; the numbers correspond to the rotational quantum number N; a, s, + and − designate the symmetry properties of the molecular states; the thin and bold lines indicate levels and transitions between levels symmetric (s) and anti-symmetric (a) with respect to interchange of the nuclei, respectively; upward and downward arrows indicate electronic excitations and optical transitions, respectively; the left-hand part of the graph shows a Q-branch of the Fulcher-α band; the right-hand part shows (exemplarily) P-, Q-, R-branches from the Π states of the 4d level into the upper Fulcher-α levels.

The thermal rotational distribution of the electronic ground state $1s\,^1\Sigma_g^+$ is 'copied' into the excited state $3p\,^3\Pi_u^-$ without change of the rotational quantum number, N, under these conditions.

The rotational population of the excited state can be determined from the spontaneous emission into the state $2s\,^3\Sigma_g^+$. In the analysis of the Boltzmann distribution for the determination of the gas temperature the rotational constant of the ground-state configuration has to be taken into account [15]. Figure 2 shows, in the left-hand part, the excitation scheme under these conditions. The levels of *ortho*-hydrogen, antisymmetric with respect to permutation of the nuclei, are designated by 'a'. The role of the transitions from the 4d states is discussed in the following section.

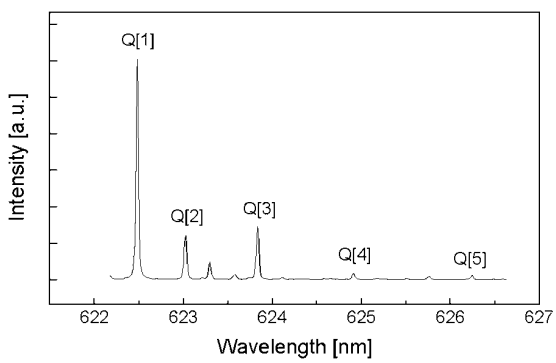

Figure 3. Spectrum of the first five rotational lines of the Fulcher-α $v = 2$ Q-branch.

4. Experimental results

4.1. Hydrogen

The usual way to determine the gas temperature on the basis of the described model is to observe the Q-transitions of the diagonal bands ($\Delta v = 0$) of the Fulcher-α system, since in this case the adiabatic approximation and, in consequence, the conditions (3)–(5) are best fulfilled [3]. This has been verified by a comparison with Doppler measurements [16]. The vibrational transition $v' = 2 \rightarrow v'' = 2$ is particularly well suited since the rotational lines have no overlap with other emission lines. With our high spectral resolution it was also possible to observe the vibrational transitions for $v' = 0, 1, 3$ and 4 with $\Delta v = 0$. We find the same time dependences and an agreement of the inferred temperatures to within 10%. Figure 3 shows a spectrum of the first five rotational lines of the $v' = 2 \rightarrow v'' = 2$ transition. It is obvious that a considerable dynamic range is necessary for this measurement in order to be able to determine the gas temperature. Since the relative error with low-intensity molecular lines is larger than for more intense ones, no linear fit was applied to obtain the temperature from a Boltzmann plot, but the least squares'

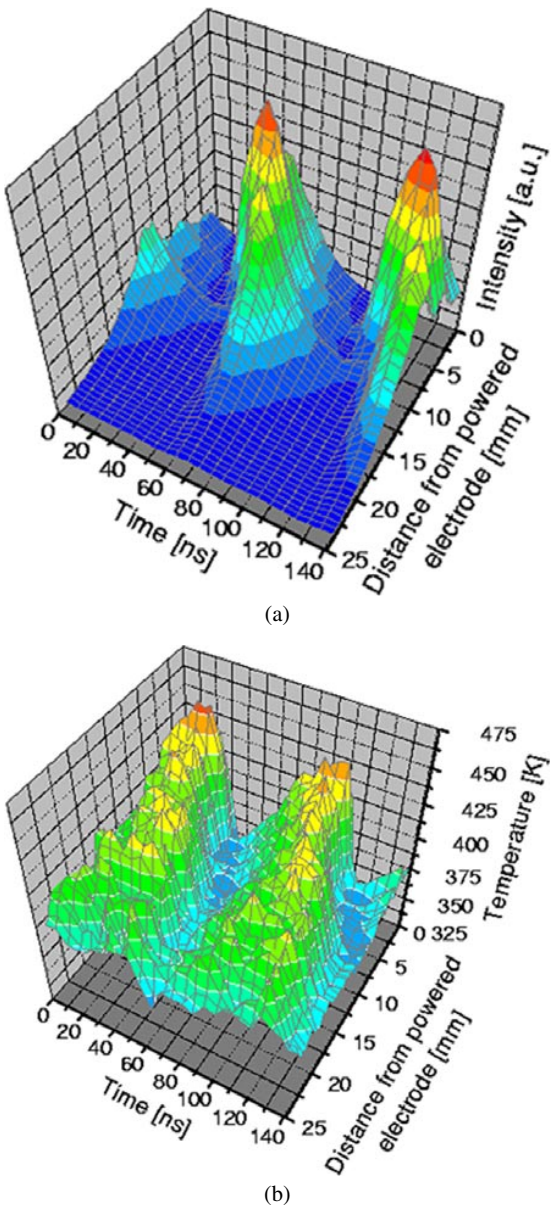

(a)

(b)

Figure 4. Time-resolved emission intensity of Q[1] (a) and rotational temperature history (b) along the discharge axis. The time axis shows two RF cycles of 74 ns each; the second space axis denotes the distance from the powered electrode at zero position; and the temperature is determined from the first five rotational lines of the Fulcher-α Q-branch.

deviation between the calculated intensities from the model and the measured intensity was used, so that all rotational lines contribute according to their intensity. This method proved to be best suited in a test whereby spectra with relative intensities according to a given temperature were artificially subject to statistical noise.

Figure 4(a) shows two RF periods of the Fulcher Q[1] emission with the spatial resolution along the discharge axis for $p = 42$ Pa and $P = 100$ W. Two emission maxima occur in each RF cycle at different times and different distances from the powered electrode. This phenomenon was also observed at a similar discharge and was investigated by electric field measurements [6]. The explanation is that the luminous peak,

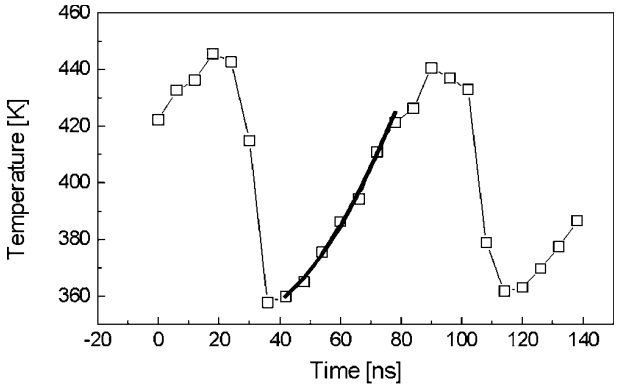

Figure 5. Comparison of the time dependences of the measured (squares) and calculated rotational temperatures in the region close to the powered electrode. The calculation starts at the time of maximum emission ($t \simeq 40$ ns; for details see text).

more distant from the electrode, is caused by an excitation by electrons expelled from the space charge sheath in front of the electrode into the plasma bulk. The second peak arises through field reversal leading, in hydrogen, to an acceleration of the electrons from the sheath edge to the electrode. The emission decays in both cases according to the effective lifetime of the excited population. The transitions Q[2] to Q[5] exhibit the same emission characteristics so that an analysis of the temperature on the basis of the model outlined can be performed with these images at any time and position between the electrodes. The result is shown in figure 4(b). The model yields apparently the lowest temperatures ($T \approx 360$ K) at times of maximum emission. After a slow rise ($\Delta T \approx 90$ K) it decays again steeply to the low value characterized by strong electron collisional excitation connected with strong emission. Since the actual gas temperature does not change on this time scale, the apparent changes have to be caused by deficiencies of the model. Among the basic assumptions listed above, only condition (2) is influenced by time dependences, so that the observed phenomenon is obviously due to a change of the rotational distribution of the upper levels. This can occur by collisions of excited molecules with other molecules or by an additional population of the excited rotational levels by cascading processes from higher states. These observations of population changes are also found at the lowest pressure, where redistribution by collisions is not likely. We will therefore consider population changes by cascade processes in the following.

Figure 2 shows how the observed excited $3p\,^3\Pi_u^-$ level can be populated in addition to direct electron collisions by cascade processes from higher states. If electrons of sufficient energy are available in the discharge, cascades can be expected as described in [17]. We expect those electrons to be present during certain times within the RF cycle in our discharge [6]. The 4d levels are expected to yield the dominant cascading contributions to the considered 3p level [18]. According to the selection rules for electronic transitions Q-transitions from $4d\,^3\Sigma_g^+$, $4d\,^3\Pi_g^+$ and $4d\,^3\Delta_g^+$ states as well as P- and R-transitions from $4d\,^3\Pi_g^-$ and $4d\,^3\Delta_g^-$ states are considered. It is reasonable to assume that they are of comparable intensity in our case. Only the transitions from the Π states are shown in figure 2.

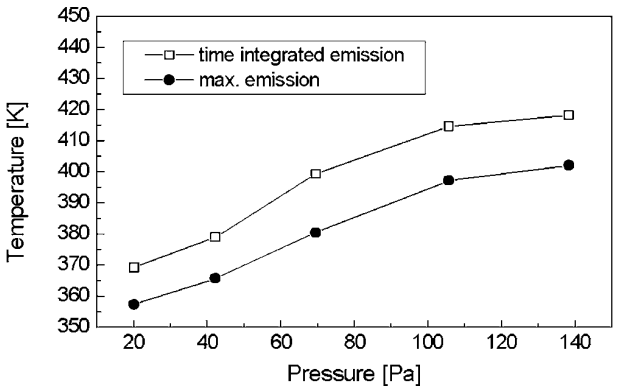

Figure 6. Comparison of gas temperatures calculated from peak intensities of time-resolved and from time-integrated measurements at different gas pressures.

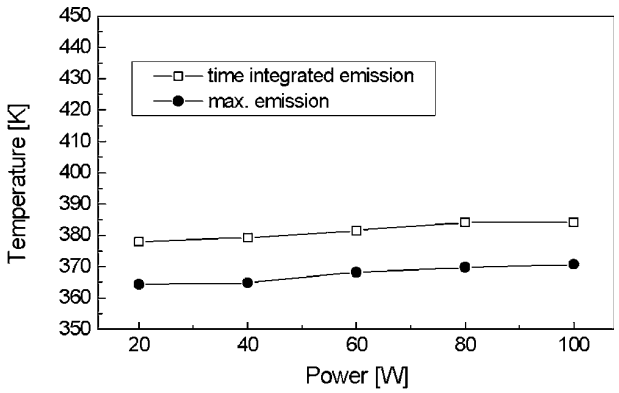

Figure 7. Comparison of gas temperatures calculated from peak intensities of time-resolved and from time-integrated measurements at different discharge powers.

A lifetime of 143 ns is reported in [17] for these cascade contributions. Our discharge has a period of 74 ns so that the cascades have only a weak time dependence. Their contribution is superimposed onto the excitation by electron collisions lasting approximately 15 ns. The influence of this cascade contribution, which is neglected in the commonly applied model for the temperature determination, is least when the emission is a maximum. The determination of the gas temperature on the basis of the described model is therefore best justified for this time interval.

A simple simulation shows that higher values are obtained for the rotational temperature along with the increasing influence of the cascading transition in comparison with direct electronic collisional excitation. This is illustrated in figure 5. The simulation starts at the maximum emission. At this time ($t \simeq 40$ ns) the population of the $3p\,^3\Pi_u^-$ level corresponds to the population distribution of the $1s\,^1\Sigma_g^+$ ground state with a temperature of 360 K. The influence of cascades is neglected at the beginning in view of the strong collisional excitation. The rotational levels are then depopulated with an effective lifetime which includes quenching; population occurs due to cascading by the transitions described. Populations by electron collisional excitation are disregarded after the initial phase. For the 4d levels no further population by secondary cascades is taken into account so that an exponential depopulation with a lifetime of $\tau = 143$ ns [17] can be assumed. The temporal development of the population $N_{N'}(t)$ of a $3p\,^3\Pi_u^-$ rotational level is described by the following rate equation:

$$\frac{\mathrm{d}}{\mathrm{d}t}N_{N'}(t) = -(A+Q)N_{N'}(t) + C(N')\exp\left(-\frac{t}{\tau}\right).$$

In this equation A describes the fluorescence rate and Q the quenching rate. The parameter $C(N')$ describes the strength of the cascading contributions. The following relation results:

$$N_{N'}(t) = N_{N'}(0)\exp(-(A+Q)t) + \frac{C(N')}{A+Q-(1/\tau)}\left[\exp\left(-\frac{t}{\tau}\right) - \exp(-(A+Q)t)\right].$$

The dependence of the cascading contributions $C(N')$ on the rotational quantum number N' is determined by the dependence of the transition probabilities from the 4d levels into the 3p levels and the rotational distribution of the 4d levels. The transition probabilities are given in adiabatic approximation by the Hönl–London factors which are given in [19] for the transitions considered here. The rotational distribution in the upper levels due to electron collisional excitation from the ground state is described by the following expression [20]:

$$N_{n'v'N'} \propto Y_{n'\leftarrow n''}(T_g, N')g_{a,s}(2N'+1) \times \exp\left(-\frac{N'(N'+1)B_0}{kT_g}\right).$$

In this equation B_0 is the rotational constant of the ground state and $Y_{n'\leftarrow n''}(T_g, N')$ describes the dependence of the excitation rates on the rotational quantum number. $Y_{n'\leftarrow n''}(T_g, N')$ depends on the electronic state considered and can be expressed with the aid of Wigner's 3-j symbols in adiabatic approximation [18, 21] for the states $4d\,^3\Sigma_g^+$, $4d\,^3\Pi_g^+$and $4d\,^3\Delta_g^+$ with $\Delta N = 0$ in the following manner:

$$Y_{n'\leftarrow n''}(T_g, N') = (2N'+1)\begin{pmatrix} N' & 2 & N' \\ -\Lambda' & \Lambda' & 0 \end{pmatrix}^2.$$

Here Λ' is the angular momentum about the internuclear axis in the excited state. The 'zero' in the 3-j symbol stands for $\Lambda'' = 0$ in the ground state; the 'two' is valid for the considered transitions from 1s to 4d. The following expression results for the states $4d\,^3\Pi_g^-$ and $4d\,^3\Delta_g^-$ with $\Delta N = \pm 1$ due to the two contributions where the rotational quantum number changes:

$$Y_{n'\leftarrow n''}(T_g, N') = (2N'-1)\begin{pmatrix} N' & 2 & N'-1 \\ -\Lambda' & \Lambda' & 0 \end{pmatrix}^2 \times \exp\left(\frac{2N'B_0}{kT_g}\right) + (2N'+3)\begin{pmatrix} N' & 2 & N'+1 \\ -\Lambda' & \Lambda' & 0 \end{pmatrix}^2 \times \exp\left(-\frac{(2N'+2)B_0}{kT_g}\right).$$

With the given formula for the temporal development of the population of the rotational levels, both the temporal behaviour of the emission and the history of the temperature can be determined on the basis of the comparison of all rotational lines with the model described. The lifetime of the cascading transitions was not treated as a fitted parameter but is taken as a constant (143 ns) since its influence is relatively small in view of the duration of a discharge cycle.

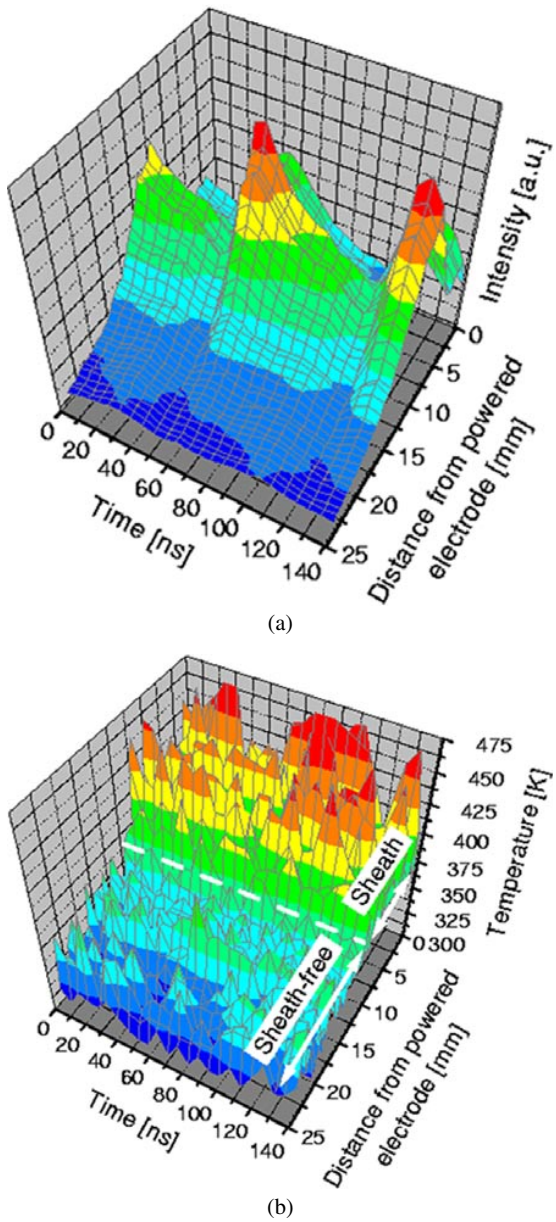

Figure 8. Time-resolved emission (a) and gas temperature (b) determined from the first negative system of $N_2^+(v = 0;\ \Delta v = 0)$. The temperature determination is meaningful only within the sheath-free region where the ions are not influenced by the electric field of the sheath. The time and space axes are as figure 4.

The strength of the cascade contributions considering their dependence on the rotational quantum number and the effective lifetime $1/(A + Q)$ are treated as fitted parameters. The time dependence of the temperature is strongly influenced by the strength of the cascades, whereas the temporal behaviour of the emission depends strongly on the effective lifetime. The self-consistent solution represented in figure 5 results after iteration of the fitted value for the effective lifetime to obtain the time dependence of the emission, and of the fit for the strength of the cascades to describe the temporal development of the temperature. For $A + Q$ a value of $6.1 \times 10^7\ s^{-1}$ is obtained. This leads to a self-quenching coefficient k_{H_2} of the considered upper Fulcher levels of $k_{H_2} = Q/n_{H_2} = 4.3 \times 10^{-9}\ cm^3\ s^{-1}$ at 360 K, a pressure of 42 Pa and for a fluorescence rate of $A = 2.5 \times 10^7\ s^{-1}$ [3]. This is in good agreement with the value obtained by Burshtein *et al* [22] of $4.5 \times 10^{-9}\ cm^3\ s^{-1}$ at 600 K. The contribution of the cascades within an RF-cycle amounts to 8.4% in relation to electron collisional excitation. A value of this order was expected on the basis of the results communicated in [17, 18].

Figures 6 and 7 show a comparison of the temperature analysis at the time of maximum emission with time-integrated measurements. In the figures both the pressure and power dependences are shown. The temperature shown is the mean value in the discharge volume. The time-averaged measurements yield, in all cases, values that are higher by approximately 15–20 K than the values obtained at the maximum emission. This is due to the fact that the time-integrated measurement also includes intensities that are generated in the discharge during times when the model assumptions are not satisfied. The fact that the deviation is independent of pressure indicates that the population changes in the excited state are not due to collisions. Deviations are comparable to the statistical error and amount to about 5% with a measurement time of 30 min; they are, however, systematically present within all measurements. For most technical applications of hydrogen plasmas this deviation can very likely be neglected, with the possible exception of surface modifications of sensitive polymers or membranes. The observation that the gas temperature is almost independent of the power supplied can be understood by the expansion of the discharge volume with increasing power, so that the power is distributed over a larger plasma volume. The measured increase of the neutral gas temperature with pressure can be understood in terms of the higher plasma density (measured by microwave interferometry [23]) and higher collisional frequency at an elevated pressure. This leads to a more efficient energy transfer between the energetic ions within the sheath and the neutral gas [6, 24].

4.2. Nitrogen

Rotational bands of molecular nitrogen or of N_2^+ are also well suited to the spectroscopic determination of the gas temperature [10, 11]. The question arises whether similar cascade effects as found for hydrogen are also present in the case of nitrogen. The neutral nitrogen bands were too weak in our experimental situation to yield sufficient intensity. We investigated, therefore, the rotational band $B\,^2\Sigma_u^+(v = 0) \rightarrow X\,^2\Sigma_g^+(v = 0)$ of the first negative system of N_2^+ around $\lambda = 390$ nm. The lifetime of the ionic B states is approximately 65 ns [25].

A calculated spectrum was adapted to the recorded emission spectra in order to obtain the temperature. The lines (both spectral position and relative intensity) of this synthetic spectrum were obtained with the aid of molecular constants published by Herzberg [19]. The calculated lines ($J_{max} = 40$) of the P- and R-branches were convolved with an experimentally determined instrumental profile.

In analogy to the procedure for hydrogen, a rotational temperature is determined with spatial and temporal resolution. The results can, however, only be used for the region in the discharge outside the sheath because of the influence of the electric field in the latter. Within the sheath, the ions

are accelerated by the electric field and are not in thermal equilibrium with the neutrals. As shown in figure 8(b), the temperature determined from these N_2^+ lines does not exhibit a temporal dependence although the pertaining emission profiles exhibit a similar behaviour to that observed in the case of hydrogen. This is outlined in figure 8(a).

We conclude that in the case of these N_2^+ emission spectra, no redistribution by cascading transitions is present. This is not surprising since (unlike the H_2 case) only one level ($D\,^2\Pi_g$) is a candidate for cascading [25]. The N_2^+ temperatures deviate in all cases by less than 10% from the H_2 temperatures.

5. Summary

We report on time-resolved spectroscopic measurements of rotational state populations over a full cycle of an RF discharge plasma. This allows us to critically analyze the model assumptions for the determinations of the plasma parameters on the basis of commonly used models. The rotational bands of the Fulcher-α emission were analysed in order to examine the commonly used method of gas temperature measurements based on time-integrated emission. A substantial temporal variation of the population distribution of the upper levels was observed, from which one can infer a temporal variation of the gas temperature over an RF cycle. This change in the rotational population can be explained by cascading effects from higher electronic states. A simple model was developed which supports this argument. This time-dependent model yields the result that the commonly used time-independent model is correct when applied to the time interval of maximum emission. A comparison of the time-integrated measurements of the rotational populations and the determination of the gas temperature on this basis and analogous measurements on the basis of the population distribution obtained for the time of the emission maximum within the cycle show a small systematic error of the first method. We conclude that in most practical cases the time-integrated measurements yield the gas temperature with sufficient accuracy. In the case of N_2^+ similar effects are not observed.

Acknowledgments

We thank Mrs C Fischer and Mr J Leistikow for skillful technical assistance. Support by the 'Deutsche Forschungsgemeinschaft' in the framework of Sonderforschungsbereich 191 is gratefully acknowledged.

References

[1] Liebermann M A and Lichtenberg A J 1994 *Principles of Plasma Discharges and Materials Processing* (New York: Wiley)
[2] Schulz-von der Gathen V and Döbele H F 1996 *Plasma Chem. Plasma Process.* **16** 461
[3] Astashkevich S A, Käning M, Käning E, Kokina N V, Lavrov B P, Ohl A and Röpcke J 1996 *J. Quant. Spectrosc. Radiat. Transfer* **56** 725
[4] Malyshev M V and Donnelly V M 1999 *Phys. Rev.* E **60** 6016
[5] Hori T, Kogano M, Bowden M D, Uchino K and Muraoka K 1998 *J. Appl. Phys.* **83** 1909
[6] Czarnetzki U, Luggenhölscher D and Döbele H F 1999 *Plasma Sources Sci. Technol.* **8** 230
[7] Mahony C M O and Graham W G 1999 *IEEE Trans. Plasma Sci.* **27** 72
[8] Radovanov S B, Olthoff J K, Van Brunt R J and Djurovic S 1995 *J. Appl. Phys.* **78** 746
[9] Hargis P J *et al* 1994 *Rev. Sci. Instrum.* **65** 140
[10] Muntz E P 1962 *Phys. Fluids* **5** 80
[11] Behringer K 1991 *Plasma Phys. Control. Fusion* **33** 997
[12] Lavrov B P 1980 *Opt. Spectrosc.* **48** 375
[13] Lavrov B P, Ostrovsky V N and Ustimov V I 1980 *Sov. Tech. Phys.* **50** 2072
[14] Bryukhovetskii A P, Kotlikov E N, Otorbaev D K, Ochkin V N, Rubin P L, Savinov S Yu and Sobolev N N 1980 *Sov. Phys.–JETP* **52** 852
[15] Otorbaev D K, Ochkin V N, Rubin P L, Savinov S Yu, Sobolev N N and Tskhai S N 1989 *Electron-Excited Molecules in Nonequilibrium Plasma* (Commack: Nova)
[16] Röpcke J, Käning M and Lavrov B P 1998 *J. Physique* IV **8** 207
[17] Day R L and Anderson R J 1978 *J. Chem. Phys.* **69** 5518
[18] Baltayan P and Nedelec O 1975 *J. Physique* **36** 125
[19] Herzberg G 1950 *Spectra of Diatomic Molecules* (Princeton, NJ: Van Nostrand-Reinhold)
[20] Lavrov B P and Tyutchev M V 1984 *Acta Phys. Hung.* **55** 411
[21] Lavrov B P, Ostrovsky V N and Ustimov V I 1981 *J. Phys. B: At. Mol. Phys.* **14** 4389
[22] Burshtein M L, Lavrov B P, Melnikov A S, Prosikhin V P, Yurgenson S V and Yakovlev V N 1990 *Opt. Spectrosc.* **68** 166
[23] Lukas C, Müller M, Schulz-von der Gathen V and Döbele H F 1999 *Plasma Sources Sci. Technol.* **1** 106
[24] Surenda M and Graves D B 1991 *IEEE Trans. Plasma Sci.* **19** 144
[25] Huber K P and Herzberg G 1979 *Molecular Spectra and Molecular Structure* vol 4 (Princeton, NJ: Van Nostrand-Reinhold)